Dynamic Nuclear Polarization using Electron Spin Cluster with Asymmetric Polarization Elevation

Raj K. Chaklashiya,[*,†] Asif Equbal,[*,‡,¶] Andrey Shernyukov,[*,§] Yuanxin Li,[*,‖] Karen Tsay,[*,‖] Victor Tormyshev,[*,§] Elena Bagryanskaya,[*,§] and Songi Han[*,⊥,#]

†*Materials Department, University of California, Santa Barbara, Santa Barbara, CA 93106, United States*

‡*Department of Chemistry, New York University Abu Dhabi, PO Box 129188, Abu Dhabi, United Arab Emirates*

¶*Center for Quantum and Topological Systems, NYUAD Research Institute, New York University Abu Dhabi, PO Box 129188, Abu Dhabi,UAE*

§*N.N. Vorozhtsov Novosibirsk Institute of Organic Chemistry SB RAS, Novosibirsk 630090, Russia*

‖*Department of Chemistry & Biochemistry, University of California, Santa Barbara, Santa Barbara, CA 93106, United States*

⊥*Department of Chemistry, Northwestern University, Wilmette, IL 60208, United States*

#*Department of Chemical Engineering, University of California, Santa Barbara, Santa Barbara, CA 93106, United States*

E-mail: rchaklashiya@ucsb.edu; asif@nyu.edu; andreysh@nioch.nsc.ru; yli05@ucsb.edu; ktsay@ucsb.edu; torm@nioch.nsc.ru; egbagryanskaya@nioch.nsc.ru; songi.han@northwestern.edu

Abstract

Dynamic Nuclear Polarization (DNP) utilizing Electron Spin Clusters to achieve resonance matching with the nucleus and to generate an Asymmetric Polarization Elevation (ESCAPE-DNP, or ESC-DNP for short) by monochromatic microwave irradiation at a select frequency is debuted as a promising mechanism to achieve NMR signal enhancements with a wide design scope requiring low microwave power at high magnetic field. In this paper, we present the design for a trityl-based tetra-radical (TetraTrityl) to achieve DNP for ^{1}H NMR at 7 Tesla, supported by experimental data and quantum mechanical simulations. A slow relaxing ($T_{1e} \approx 1$ ms) four electron spin cluster is found to require at least two electron pairs with e-e distances of 8 Å or below to yield any meaningful ^{1}H ESC-DNP NMR enhancement, while squeezing the rest of the e-e distances to 12 Å or below gives rise to near maximum ^{1}H ESC-DNP-NMR enhancements. For the more common case of a fast-relaxing spin cluster ($T_{1e} \approx 1$ μs), efficient ESC-DNP is found to require an asymmetric ESC that contains a cluster of strongly coupled narrow-line radicals coexisting with a weakly coupled narrow-line radical acting as a sensitizer to extract polarization from the cluster. This study highlights the untapped potential of utilizing strong coupling of narrow-line radical clusters to achieve microwave power-efficient DNP that extends design options beyond what is available today and offers great tunability at high magnetic field.

Dynamic Nuclear Polarization (DNP) using multiple electron spins is a powerful way to take advantage of the coupling between multiple electrons for detection of nuclei by NMR signal amplification. A key example of this, Cross Effect (CE)-DNP, utilizes two coupled electrons coupled to one nuclear spin to undergo net energy conserving cross relaxation and has found use for studying a wide variety of systems at extremely high sensitivity, including the detection of analytes for pharmaceutical components in cells at hundreds of nM concentration[1,2] and characterization of organics in environmental samples at natural abundance.[3,4] CE-DNP achieves this with relatively low microwave power requirements compared with Solid Effect (SE)-DNP due to its higher polarization transfer efficiency from electrons to nuclei caused by resonance matching of the electron spins with a nuclear spin via the triple flip ($|\omega_{e1} - \omega_{e2} = \omega_{1H}|$) matching condition. The success of CE-DNP in biradicals is dependent on the magnitude of the polarization gradient, which can be induced by microwave irradiation and tuned by the microwave power and pulse shaping capability of microwave irradiation[5,6] of a sub-set of spin ensembles generated by the g-anisotropy of the polarizing agent that in turn depends on the chemical structure. The design scope for organic biradicals to meet the cross effect DNP condition has been extensively explored, generating a handful of commercially available biradicals and another dozen or so custom biradicals for different applications, but the potential for going much beyond the current capabilities is limited.[7] CE-DNP still becomes inefficient at higher magnetic fields where fewer spins fulfill the triple flip matching condition and e-e couplings (tens of MHz) become smaller relative to the external field, resulting in a lower Landau Zener (LZ) transition probability and therefore lower polarization transfer efficiency; these effects result in higher microwave power requirements.[8] Hence, the search for DNP mechanisms that are more efficient at high fields and with low power requirements is much needed to further push the sensitivity boundary and application scope of NMR detection.

Multi-electron radical systems composed of narrow-line (small g-anisotropy) radicals forming an Electron Spin Cluster (ESC) can readily give rise to an Asymmetric Polarization Elevation (APE)

by monochromatic microwave irradiation at a select frequency of the electron spin system, forming an inhomogeneously broadened EPR line. This is conducive to power-efficient DNP (ESCAPE-DNP or ESC-DNP for short) and offers broad design scope at high magnetic field. Rather than achieve resonance matching via g-anisotropy, ESC-DNP relies on a strong multi-electron coupling network that is frequency-broadened or shifted by greater margins when more than two electron spins are coupled by dipolar, J, or both couplings. The frequency broadening by multi-electron spin coupling can easily encompass the nuclear Larmor frequency and produces a polarization gradient (referred to as APE above) upon microwave irradiation of the inhomogeneously broadened EPR line.[9,10] It is important to note that for such a polarization gradient to exist, the spin network cannot be so strongly coupled to form a "homogenous bath" but rather includes dipolar anisotropy as an essential feature to maintain a polarization gradient during microwave irradiation, whether it arises from anisotropic coupling, anisotropic relaxation, or summation of many different dipolar orientations with respect to the external field. This dramatically increases the design scope by providing the use of e-e distances between all electron spins of the cluster as variables. For example, the isotropic dipolar coupling constant between a pair of electron spins alone can (with all orientations considered) reach 300 MHz at 7 Å, 450 MHz at 6 Å distances, or 850 MHz at 5 Å (Figure S15). For simplicity, throughout this paper we refer to the absolute value of the dipolar coupling when no sign is indicated. A narrow EPR line removes the limitations owing to g-anisotropy at higher field and is much easier to saturate, while the strong dipolar coupling compensates for the lower LZ transition probability for the triple spin flips at higher field; these factors give ESC-DNP great potential at high magnetic field.

The challenge of using electron spin clusters (ESCs) for DNP is their short electron relaxation times (T_{1e}) that could render them EPR-silent and therefore non-saturable, quenching the DNP effect. The solution that we propose to this conundrum is the extraction of polarization from the "invisible" or hard to detect electron spin cluster via coupling to a more isolated narrow-line radical (a "sensitizer") for read-out. The typically long relaxation times of narrow-line radicals

allow for power-efficient saturation and hence can maintain a polarization gradient between their saturated and non-saturable ESC populations. By fulfilling resonance matching through the coupling to a frequency-broadened non-saturable ESC, with the frequency difference between the narrow and broad line encompassing the nuclear larmor frequency, they serve as sensitizers by extracting polarization from the ESCs towards the narrow-line electron spins, and hence polarize the nuclear spins (requiring the electron flip-flop to give rise to a directional flow of polarization). The sharp contrast in relaxation times between the sensitizer and the clustered radical can give rise to a positive or negative absorptive central DNP profile feature via the truncated Cross Effect (tCE).[11,12,13] Such an absorptive feature is advantageous for NMR signal amplification under MAS where the positive and negative dispersive features could otherwise cancel out due to oscillatory broadband irradiation of the entire EPR spectrum, unless special pulse sequences and irradiation schemes and timings are employed. These qualities give ESC-DNP even further design scope and potential for efficient enhancement at high fields with low power. For simplicity, in this paper the more general ESC-DNP term will be used to refer to both general cases of ESC-DNP and sensitizer-based ESC-DNP that is a close cousin to tCE (except tCE can be invoked with other fast relaxing paramagnetic species than ESC) unless differentiating between the two becomes essential.

The current method of preparing spin clusters that contain strong e-e spin coupling to achieve resonance matching for ESC-DNP is to use high concentrations of narrow-line radicals that tend to generate heterogeneous electron spin clusters.[14] Examples include the use of clustered narrow-line Trityl-OX063 found at (nominal) 40-100 mM concentration,[14] BDPA at 40-60 mM concentration,[15] and a significant fraction of P1 centers[16] that we and others have found in a recent study to be abundantly present as exchange-coupled clusters in HPHT type Ib diamond regardless of its nominal concentration. The mechanism behind multi-electron spin DNP by resonance matching using an electron spin cluster of narrow-line species has been referred to as thermal mixing (TM) DNP when using Trityl and either as thermal mixing DNP or Overhauser effect (OE) DNP when using BDPA.[15,17] While the concept of OE-DNP is orthogonal to TM-DNP, ESC-DNP is a sub-

set of TM-DNP with an emphasis on the use of strongly coupled narrow-line ESCs. While all of these examples have demonstrated ESC-DNP by increasing radical concentration via stochastic clustering, such random clustering does not help us gain a better understanding or control over the multi-electron geometry to optimize resonance matching for DNP. The use of high radical concentration can also give rise to unwanted heterogeneity of radical distribution,[18] nuclear depolarization,[19] and faster nuclear relaxation times.[20]

To resolve these issues, in this study we explore the potential of ESC-DNP primarily using a geometrically well-defined 4-electron spin cluster ("designed ESC-DNP"). To this end, we start with testing a 4-electron geometry, TetraTrityl, that has been recently synthesized from four MonoTrityl "linkers" tethered together, with e-e dipolar coupling strong enough to be detectable through EPR multiquantum spin counting experiments.[21] The TetraTrityl along with its fundamental MonoTrityl unit are shown in Figure 1ab. Both DFT (Density Functional Theory) and MD (Molecular Dynamics) were performed in order to determine possible structures that TetraTrityl adopts under experimental conditions. Both DFT and MD methods suggest that the adjacent e-e distances are of the order of 1-2 nm as shown in Figure 1cd and are explained further in the "Quantum Mechanical Simulations for ESC-DNP" section. This paper presents experimental DNP and EPR measurements of TetraTrityl in conjunction with a series of Spinevolution quantum mechanical simulations of a diverse set of ESCs[22] to determine what kind of electron geometry is necessary to yield optimal ESC-DNP enhancements with low microwave power.

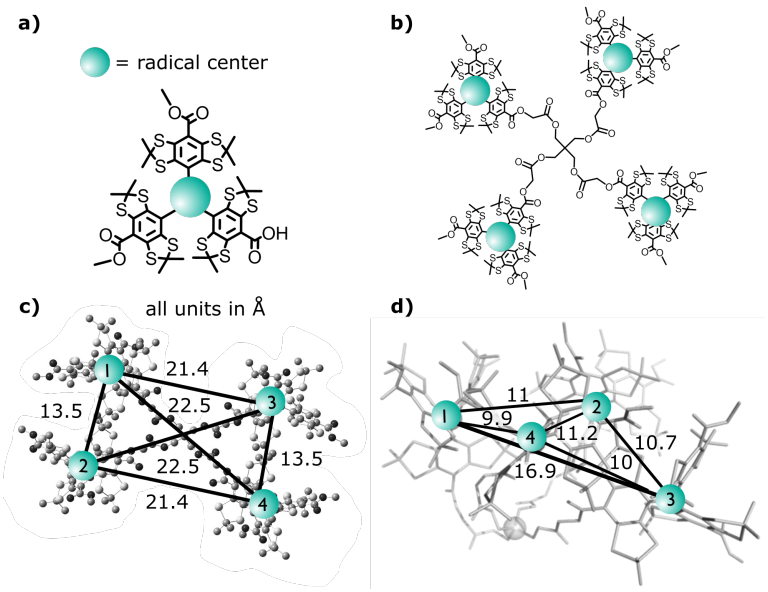

Figure 1: a) MonoTrityl radical with one electron. Green circles denote radical centers for a) - d). b) TetraTrityl radical with four MonoTrityl linkers. c) DFT-derived structure for TetraTrityl radical. d) A possible characteristic structure for the TetraTrityl radical based on MD simulations (incorporating dynamics). Tables denoting the coordinates of the radical centers and the e-e distance between any two electron pairs in c) and d) are shown in Table S8-S9.

The signs of ESC-DNP include a central feature in the DNP frequency profile, a narrow dipolar-broadened EPR line, and an enhancement vs microwave power curve showing a plateau.[15] These experiments were performed using a dual EPR-DNP setup at 6.9 T on a TetraTrityl sample at 5 mM radical concentration (20 mM electron spin concentration) in 100% protonated anhydrous toluene at 58 K, and the results are shown in Figure 2.

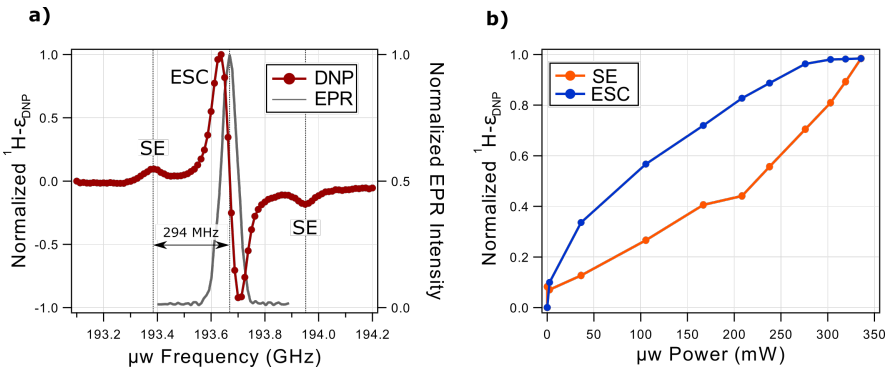

Figure 2: a) Normalized TetraTrityl DNP Profile (red) & EPR Profile (gray). Experimental ^{1}H ϵ_{DNP} vs μW Frequency at 7 T, 58 K static condition is measured for 5 mM radical concentration in fully protonated anhydrous toluene using 350 mW microwave power, 32 scans, and 7 s buildup time. The solid effect peaks are denoted with "SE" while the ESC-DNP peak is denoted as "ESC." The echo-detected EPR profile is taken in the same conditions. The difference in microwave frequency between the SE peak and center of the EPR line is noted. Actual peak enhancement for ESC-DNP is 3.2x (see discussion). b) Normalized ^{1}H DNP Power Curve for 5 mM TetraTrityl in anhydrous toluene at 58 K: DNP Enhancement as a function of microwave power at source, for the ESC and SE peaks.

A highly dispersive central feature was observed in the DNP profile, with two additional enhancement humps at $\pm$294 MHz away from the center, as seen in Figure 2a (red). The EPR profile was also measured under the same condition and shown in Figure 2a (gray), showing a narrower EPR line than the proton Larmor frequency. The normalized DNP enhancement versus power for the central and the side features is displayed in Figure 2b, showing a faster enhancement saturation for the central peak than for the side peak.

This data can be used to identify what DNP processes are happening in the sample. The two small humps in the DNP profile can be attributed to the Solid Effect (SE) as they are at $\pm$ the nuclear Larmor frequency from the center of the EPR line. The central feature could be either due to CE-DNP or ESC-DNP. Both effects can be efficient, but they utilize different processes to achieve resonance matching. CE-DNP achieves the energy difference between two (as opposed to many) coupled electron spins that typically originates from their g-anisotropy to match the nuclear Larmor frequency, while ESC-DNP can achieve matching by strong coupling within electron spin clusters that shifts or broadens the EPR frequency by the nuclear Larmor

frequency. Since the EPR spectrum is narrower than the proton larmor frequency, this rules out resonance matching by g-anisotropy, and instead ESC-DNP should be the mechanism. In other words, the energy for the nuclear spin flips is taken from a strong electron dipole-dipole reservoir.

The DNP enhancement observed using 5 mM TetraTrityl was only 3.2-fold (Figure S8, Table S4). This enhancement is very low compared to ^{1}H DNP that can be achieved with simply Trityl-OX063 monoradicals at this concentration (20 mM).[14] This low enhancement was persistent, independent of the ^{1}H concentration of the glassing solvent (30% to 100%). There are other possible causes, such as the dissolved paramagnetic oxygen in toluene solvent that makes both proton and electron spin relaxation very fast, hence impeding spectral diffusion, but cannot be solely responsible for the low DNP efficiency. For the given system, it appears that the current TetraTrityl sample formulation is far from optimal for DNP, but still clearly demonstrates ESC-DNP, which can now be studied further for optimization.

While it is clear that ESC-DNP is occurring, it is not clear whether it arises from an isolated TetraTrityl due to its four-electron geometry (designed ESC-DNP) or from clustering of Tetra-Trityl radicals (stochastic ESC-DNP). In order to distinguish between these two possibilities, DNP profiles of TetraTrityl acquired at both 5 mM and 1 mM radical concentration are normalized and compared in Figure 3a.

From the figure, it appears that while at 5 mM radical concentration, ESC-DNP is dominant as shown by the huge dispersive peak-vs-SE peak enhancement ratio (8.5x), the result for the 1 mM sample is very different: here the SE peaks are at comparable enhancement level to the dispersive peak (1.4x). A similar though less dramatic trend is also observed in 5 mM vs 20 mM MonoTrityl which supports this observation (Figure S6-S7) that intermolecular interactions, even between MonoTrityl radicals, enhance the central DNP feature relative to the SE DNP amplitude. The observation that the ESC-DNP effect is getting stronger with increasing radical concentra-

tion suggests that intermolecular e-e couplings play a dominant role in ESC-DNP. These results indicate that the TetraTrityl radical gives rise to ESC-DNP from stochastic interactions including intramolecular multi-electron coupling and intermolecular clustering in toluene.

In order to provide more definitive evidence of molecular clustering in these radicals, the presence or extent of instantaneous diffusion was determined by measuring echo-detected EPR frequency profiles at Q-band as a function of interpulse delay at low radical concentration (200 μM) and at high, DNP-relevant, concentrations (5 mM). Instantaneous diffusion is an artificial pulse-induced spin diffusion phenomenon that occurs when pulses excite electron spins of similar resonance frequency that are dipolar coupled to each other, causing them to alter each others' resonance frequency via their local fields and resulting in faster dephasing[23].[24] The results of these experiments are shown in Figure 3b-c.

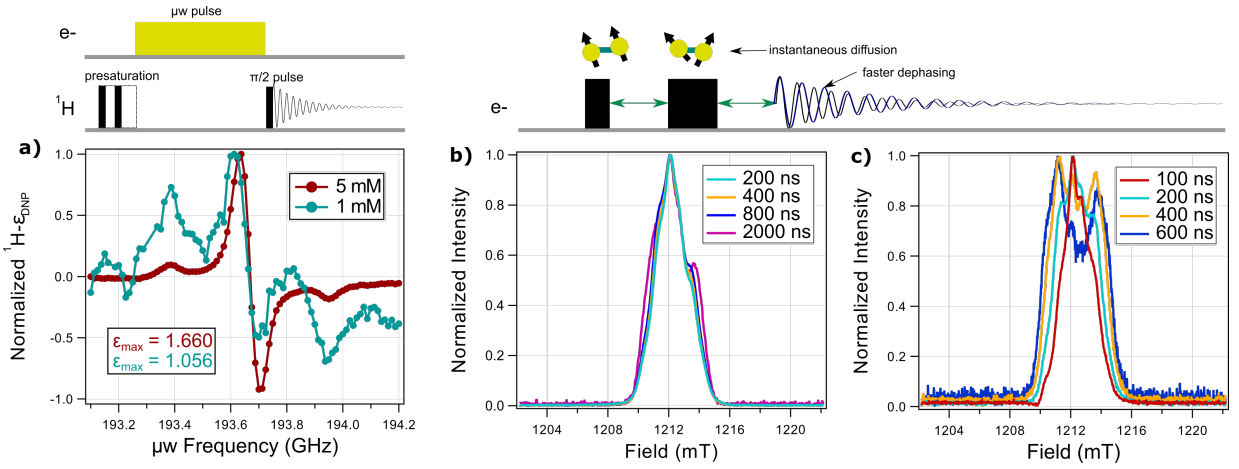

Figure 3: a) (top) Pulse sequence for DNP profiles taken on the 6.9 T static system. On top is the microwave frequency channel where a microwave pulse (yellow) at DNP buildup time length is used. On the bottom is the radio frequency channel where NMR pulses (black) are used and NMR is measured. A presaturation loop occurs before the microwave pulse, and a single ^{1}H pulse is used after the microwave pulse to get NMR signal. (bottom) DNP Profile of 5 mM TetraTrityl vs 1 mM TetraTrityl in toluene at 7 T static conditions, 60 K. b) (top) Illustration of what happens in the pulse sequence during instantaneous diffusion. Dipolar-coupled spins dephase relative to each other due to change in local fields induced by echo pulses. Normalized Q-Band EPR Spectra for b) 200 μM TetraTrityl in anhydrous toluene and c) 5 mM TetraTrityl in toluene-d$_8$, both at 50 K using nonselective pulses (0 dB) as a function of interpulse delays in the echo. More complete data can be found in Figure S10.

In Figure 3b, echo-detected EPR spectra of the low concentration (200 μM) TetraTrityl sample are acquired as a function of interpulse delay from 200 ns to 2000 ns . The spectra are normalized and overlaid for comparison. It appears that the EPR spectrum changes very little in shape with respect to interpulse delay, with the side shoulder around 1214 mT showing the most dramatic change, and even then only at a long interpulse delay of 2 μs. Normally if electrons are far enough apart (less strong inter and intra-molecular e-e couplings), instantaneous diffusion-induced dephasing is minimal, and the EPR profile does not change with respect to increased interpulse delay.

Echo-detected EPR spectra of Tetratrityl were also measured at a higher concentration at 5 mM with interpulse delays ranging from 100 ns to 600 ns, as shown normalized in Figure 3c. Here the spectrum largely looks like a single peak at a 100 ns interpulse delay, but as the interpulse delay increases the intensity at the center of the peak decreases faster than the off-center, manifesting in a Pake-like pattern (also supported by echo decay measurements, see Figure S12 and Table S7). This is in stark contrast with the result observed with 200 μM TetraTrityl. According to the literature, this "hole-burning" phenomenon observed with the 5 mM TetraTrityl sample is a common fingerprint of instantaneous diffusion.[25,24] Spectral packets with higher spin density (i.e. at the center) are more severely affected than those with lower spin density (i.e. the shoulders), resulting in a spectrum with a center whose amplitude decays faster in comparison with its shoulders as a function of dephasing time. This unambiguously demonstrates that instantaneous diffusion is occurring in TetraTrityl at 5 mM radical concentration.

The source of the instantaneous diffusion can either be intramolecular dipolar couplings (due to the four electrons within an individual TetraTrityl molecule) or intermolecular dipolar couplings (due to electron dipolar couplings between two TetraTrityl molecules). The concentration-dependence of this phenomenon indicates that the latter is the case, given that there are negligible effects of instantaneous diffusion with the same Tetraradical at 200 μM concentration. This is also supported by the appearance of instantaneous diffusion in 20 mM MonoTrityl (Figure S10), which

cannot have any intramolecular-based instantaneous diffusion and therefore must be clustering to produce such phenomena. Likely, the intermolecular clustering of the TetraTrityl radical amplifies intramolecular couplings, and vice versa, such that the Tetraradical design still contributes to the effect. What is clear from these results is that since the observed effect is so reliant on intermolecular clustering, the intramolecular e-e distances of TetraTrityl (1-2 nm) now give us an upper bound to the maximum e-e distances needed for efficient designed ESC-DNP to occur: shorter distances than 1 nm, and therefore stronger e-e dipolar couplings, are needed.

The experimental evidence presented so far shows that strong couplings from e-e distances below 1 nm are necessary for ESC-DNP. If so, what is the range of coupling strength and corresponding molecular geometry needed to produce efficient ESC-DNP? We next performed systematic quantum mechanical simulations of primarily 4-electron spin clusters using SpinEvolution software to design an efficient spin system for ESC-DNP with low microwave power requirements. This choice is made to accurately represent the molecular system that was experimentally tested, as well as reflect how 4 electrons appears to be the minimum requirement for efficient ESC-DNP while maintaining reasonable e-e distances. The first step is to corroborate the experimental results by showing through simulations that strong intermolecular couplings from subnanometer e-e distances are necessary for the TetraTrityl structure to give rise to ESC-DNP. This is explored in Figure 4 using the geometry and e-e distances of the 4-electron cluster derived from both the DFT- and MD-derived TetraTrityl structure shown in Figure 1cd.

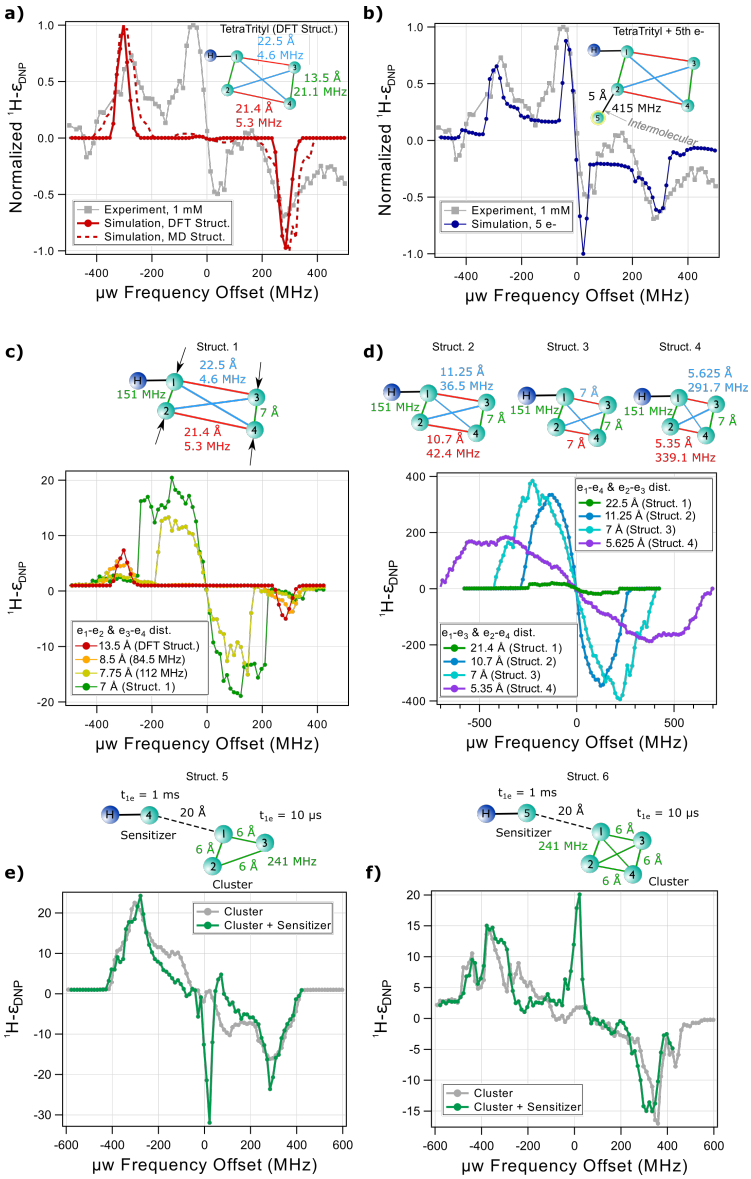

Figure 4: a) Normalized DNP profiles of TetraTrityl for the simulated DFT-derived (red, with structure in inset) and MD-derived (red-dashed, structure pictured in Figure 1D) structures, and the experimental 1 mM sample (grey). b) Normalized DNP profile comparison between simulated DFT-derived TetraTrityl with a fifth electron 5 Å away from e_2 (a clustered scenario, in dark blue, with structure pictured in inset) and experimental 1 mM TetraTrityl (gray). c) Simulated DNP profile of TetraTrityl as a function of shrinking e_1-e_2 and e_3-e_4 distance from 13 Å to 7 Å. Pictured above figure is the resulting structure for the 7 Å case, labeled "Struct. 1." d) Simulated DNP profile of Structure 1 as a function of shrinking e_1-e_3 and e_2-e_4 distances, from 21.4 Å to 5.35 Å. The e_1-e_4 and e_2-e_3 distances are also simultaneously shrinking, see Table S10. Above the figure are the new structures simulated in this figure (labeled 2-4). e) Simulated DNP profile comparison between a fast relaxing (10 μs t_{1e}) 3-spin cluster at 6 Å e-e distance (grey) and the same 3-spin cluster except with a fourth slow relaxing (1 ms t_{1e}) electron acting as a sensitizer (green, Struct. 5). f) Simulated DNP profile comparison between a fast relaxing (10 μs t_{1e}) 4-spin cluster at 6 Å e-e distance (grey) and the same 4-spin cluster except with a fifth slow relaxing (1 ms t_{1e}) electron acting as a sensitizer (green, Struct. 6). For all figures, ^{1}H-e_1 distance is 6 Å.

The DFT-derived structure of TetraTrityl takes a rhombic disphenoid form with two "short" e-e distances of 13.5 Å and two "long" e-e distances of 22.5 Å and 21.4 Å, as shown in Figure 1c. These distances were chosen as they are similar to that of nitroxides like AMUPOL (12.5 Å).[26] Molecular dynamics simulations were also performed on TetraTrityl to get more insight into one of the possible characteristic structures when accounting for dynamics (see SI Section A) with one such structure shown in Figure 1d, showing a "Bouquet-like" structural form with a smallest e-e distance of 9.9 Å. These two configurations both matter as the MD-derived structure takes into account molecular dynamics in the solvent while the DFT-derived structure provides a reasonable energy-minimized structure. The two structures explored are just a small sample of the possible conformations that TetraTrityl may take under experimental conditions (Figure S1-S3), but these structures offer the opportunity to simulate the ^{1}H DNP profile that two possible structures would yield to compare to the experimental results.

In Figure 4a, the numerically simulated DNP profile of a 4-electron 1-proton spin system with e-e geometry and coupling inspired by the DFT-derived TetraTrityl geometry (shown in solid red) and the MD-derived geometry (shown in dashed red) are compared with the experimental DNP profile of 1 mM TetraTrityl, shown in gray. Both simulations show dominant SE features, with the MD structure showing slightly broader peaks, potentially due to the higher coupling asymmetry. With both structures, the central ESC-DNP feature was not prominent. This makes sense as experiment had shown that ESC-DNP could not come from a single TetraTrityl as the e-e coupling is too weak to give rise to ^{1}H ESC-DNP in such a molecule, but from inter-TetraTrityl interactions.

To simulate the effect of molecular clustering that leads to a strong intermolecular e-e coupling, a fifth electron, 5 Å away from e_2 in the TetraTrityl structure, was added as shown in Figure 4b in dark blue compared with the gray 1 mM TetraTrityl. Remarkably, a prominent central ESC-DNP feature shows up, very similar to what was seen in the experiment. We can conclude that an individual TetraTrityl molecule does not give ESC-DNP on its own (due to relatively long

e-e distances), but that clustering with other radicals at subnanometer distances can readily give rise to ESC-DNP. Note that while a distance of 5 Å was found to produce strong ESC-DNP for this clustered TetraTrityl system, in reality TetraTrityl stacking would involve 8 electrons (for two TetraTrityls), which would allow for larger than 5 Å e-e distances to produce the same size of effect. Unfortunately, 8-electron simulations could not be performed due to exceedingly long simulation times, and hence we demonstrate the impact on ^{1}H DNP of only adding a 5th electron to the electron spin cluster to illustrate the effect of radical clustering.

In order to determine what kind of multi-electron geometry would give high ESC-DNP enhancement, we start from the DFT-derived structure and consider the effect of shorter e-e distances on the DNP profile. From both Figure 4a and Figure 4b we see that shorter e-e distances result in a larger central DNP feature (slightly larger in the case of going from DFT to MD structure for A and much larger when adding a fifth electron 5 Å away for B). To understand the effect of these e-e distances and whether there is a minimum coupling necessary to see the emergence of ESC-DNP, we systematically shrunk only the e_1-e_2 and e_3-e_4 distances (the shortest distances in the DFT structure) concurrently from 13 Å to 7 Å. A twisted lattice structure is used here, as shown in Figure S13. This shortening process is illustrated by a simplified two-dimensional projection based on the TetraTrityl design as shown in the structure labeled "Struct. 1" in Figure 4c where the e_1-e_2 and e_3-e_4 distances are shrunk down to 7 Å while initially keeping the other e-e distances the same as in the initial TetraTrityl structure.

We find that the emergence of ESC-DNP starts at a e_1-e_2 and e_3-e_4 distance of around 8 Å, growing larger at 7 Å, while SE-DNP shrinks at the same crossover point. The structure with 7.75 Å e-e distances along with Structure 1 (7 Å) appear to be the first controlled multi-electron structures that give rise to a dominant ESC-DNP over SE-DNP. The simulated data show us that even when considering molecular dynamics that permit the e_1-e_2 and e_3-e_4 distances to reach 9 Å, the closest e-e distance needs to still be 1-2 Å shorter than those values to generate efficient

ESC-DNP using a four electron spin cluster. This crossover is a sudden jump in enhancement for ESC-DNP but only a small fall in SE-DNP, as shown in Figure S14a. This sudden jump occurs even though the dipolar coupling constant exceeds a value of only 100 MHz at that point (Figure S14a), which is not enough to encompass 294 MHz and demonstrates that the effect cannot be determined by a single dipolar coupling constant value and instead requires an understanding of the contributions from multiple electron spins and their orientations as determined by the dipolar coupling equation $\omega_{dd} = d\,(1 - 3\cos^2\theta)$). For a single electron spin pair, such a distribution would begin to encompass 294 MHz at 7 Å and smaller distances (Figure S15), which makes it non-trivial to explain the emergence of ESC-DNP at 8 Å in the 4-electron spin cluster. This observation implies that the effect is dependent on the presence of multiple strong electron couplings, which is difficult to model analytically but can be demonstrated through the use of quantum mechanical simulations of the EPR spectra of various ESCs. The simulations (Figure S14bc) show that the transition from SE DNP to ESC DNP occurs as the EPR linewidth exceeds 294 MHz at 30% of its height, giving ample room for enough e-e spin packets to fulfill the resonance matching condition with the nuclear larmor frequency and hence produce ESC-DNP. This approach is backed up by studies of a dipolar coupling-based cut-off frequency to determine the efficiency of ESC-DNP.[27,28,29] It is noteworthy that the crossover from dominant SE DNP to ESC DNP occurs at an e-e- distance below 7 Å (Figure S15ab) in a simpler 3-electron spin system with only one strongly coupled spin pair (Figure S16-S17). This means that having more than one strongly coupled spin pair invokes increased flexibility for e-e distances necessary to produce resonance matching conditions for the ESC-DNP effect.

This ESC-DNP can be further optimized by now taking the Structure 1 and shortening the rest of the e-e distances as shown in Figure 4d and Table S10. When the e_1-e_3 and e_2-e_4 distance is 10.7 Å (blue), the ESC-DNP enhancement increases almost 20-fold as compared with Structure 1. This is dubbed Structure 2. As one moves down to 7 Å e-e distances all around, one finds that the enhancement increases gradually, reaching a peak of around 400-fold (Structure

3, turquoise DNP profile with structure shown in inset). Shrinking the distance to shorter than 7 Å now reverses the effect and decreases the enhancement as the profile becomes significantly wider (purple). Notably, the DNP enhancement in this geometry is still 10x higher than that of Structure 1. These results show that the shortening of e-e distances to between 7-11 Å with two electron pairs at 7 Å distance yields the highest ESC-DNP enhancement, and that the critical factor that drives ESC-DNP via multi-electron geometries is the close e-e distance, requiring a shortening in e-e distance from the original DFT-derived TetraTrityl structure by a factor of about 2. These effects appear to be robust with respect to radical g-anisotropy (Figure S18) as Tetra-BDPA and Tetra-AMUPOL versions of Structure 3 appear to give similarly high DNP enhancement at the same field, and appear to be robust with respect to increasing field, as a drop of only 1-2 e-e distance for all electron pairs in Structure 3 is necessary to retain similarly high enhancements when moving up to 600 MHz and 900 MHz field (Figure S19). These results together demonstrate the design potential and power efficiency that ESC-DNP offers at high field.

The previous simulations were all performed using the experimentally found T_{1e} of TetraTrityl at 50 K, approximately 1 ms, showing us that the ideal DNP polarizing agents are those consisting of highly clustered spins with relatively long T_{1e} if designable by synthetic chemistry. The significantly wide central feature for these simulations is also attributed to this relatively long T_{1e}. In reality, electron spin clusters should have much shorter relaxation times, which negatively impacts the polarization enhancement pulled out, as shown in Figure 4e (gray) for a 3-spin cluster and Figure 4f (gray) for a 4-spin cluster, where both clusters are at 6 Å e-e distances and relaxing at 10 μs T_{1e}. In both cases, the enhancement has become much lower (approximately 15-20-fold) and is primarily due to SE-DNP.

However, in this situation one can use a slower relaxing electron spin further away to act as a sensitizer to "pull out" the polarization and enhance a nearby nuclear spin via sensitizer-enhanced ESC-DNP. This is shown in Figure 4e (green) for a 3-spin ESC + 1-spin sensitizer and Figure 4f

(green) for a 4-spin ESC + 1-spin sensitizer, where the ESC is at all 6 Å e-e distances, the 1-spin sensitizer is consistently 20 Å away from the ESC, the cluster is relaxing with a T_{1e} of 10 μs, and the sensitizer at a T_{1e} of 1 ms (these choices are made with insight from simulated EPR profiles shown in Figure S20). In the cases where a sensitizer is added, one can see a return of the central feature, except now much narrower than in Figures 4cd and absorptive in nature, and that this central feature is higher than the SE intensity (20-30-fold enhancement). Still, the addition of a sensitizer cannot completely recover the hundreds-fold enhancement of the slow relaxing ESC models of Figures 4cd. The absorptive nature of the central feature is due to this now being an example of ESC-DNP that utilizes the tCE where the polarization differential between fast relaxing and slow relaxing populations results in a shift in the EPR line. These results demonstrate the potential of slow-relaxing sensitizer radicals to extract hidden polarization from fast-relaxing ESC. Efforts to determine the optimal sensitizer-cluster geometry for recovering the hundredfold enhancement of slow-relaxing ESC are underway but outside the scope of this study.

These findings are promising as they demonstrate a regime where e-e distances can be tuned to achieve optimal designed ESC-DNP, and in cases where clusters are fast-relaxing, to recover part of the enhancement via a slow-relaxing and narrow-line radical as the sensitizer. Efforts to build a new electron spin cluster system based on the new design principles derived in this work are underway, but these studies are outside the scope of this work since the desired cluster system needs to be synthesized first.

This manuscript explores the design principles necessary for achieving resonance matching for efficient ESCAPE-DNP at high magnetic field and with low microwave power requirements. Experiments of a TetraTrityl (a 4-electron spin system) at 7 T with e-e distances at typical biradical linker length of 1-2 nm showed the occurrence of ESC-DNP through the observation of a dispersive central feature in the DNP profile. However, concentration-dependent DNP and EPR experiments demonstrated that this dispersive feature comes mostly from intermolecular e-e

couplings (molecular stacking of TetraTrityl) rather than intramolecular e-e couplings (isolated TetraTrityl). These results confirmed that subnanometer e-e distances are necessary to induce efficient ESC-DNP with resonance matching at high magnetic fields. The experimental results were verified by quantum mechanical DNP simulations. Additionally, in-silico design of TetraTrityl revealed that at least two e-e pairs must be 7 Å or smaller distance apart for ESC-DNP to emerge from an isolated TetraTrityl so that the span of dipolar coupling is large enough to encompass the nuclear larmor frequency. Optimal ESC-DNP emerges as the rest of the e-e distances are further shrunk to below 12 Å and is relatively robust with respect to increasing field and radical g-anisotropy. Even when fast relaxation of such a cluster obscures any observable DNP effect, ESC-DNP via a sensitizer electron spin is found to recover DNP enhancement. These results can serve as design principles for synthesis of efficient ESC-DNP polarizing agents at high field through molecular assembly methods. The parameter space for optimal ESC-DNP is very wide, as increasing number of electrons, changing e-e distances, and incorporating exchange coupling can all increase the possible electron spin geometries yielding efficient ESC-DNP with resonance matching. This study's results can also readily be applied to the investigation of multi-electron effects in important materials for quantum information science, such as defect centers in diamonds and semiconductors and spin-based multiqubit quantum systems.

Experimental and Computational Methods

Molecular dynamics simulations were performed via the Amber20[30] software package using GAFF force field (Version 1.81). For trityl moieties, force field parameters obtained previously[31] were used. Charge derivation was made by AM1-BCC method with sqm and Antechamber utilities included in the package AmberTools21.[30] Simulations were run for the major symmetrical isomer with the MMPP trityl propellers configuration.[32] Sampling of the conformational space was carried out in two stages using plain molecular dynamics *in-vacuo* (Langevin dynamics with collision frequency 1 ps^{-1} with Coulomb cut-off distance 12 Å.) Annealing details are described in the SI.

Sample preparation for pulsed Q-Band and 7 T DNP is as follows. About 1 mg of powder sample is first weighed and then added to an eppendorf tube. Solvent is then added to the tube, then the sample is vortexed and centrifuged until homogeneous. It appears as a dark green liquid. Lower concentration sample is formed by diluting the higher concentration sample, resulting in a lighter green sample color. The samples were not degassed because Trityl is highly stable in contact with oxygen compared to other radicals such as BDPA.

For Q-Band EPR samples, 5 uL of sample is pipetted into an EPR tube, which is then further shortened to minimize air volume. The tube is then sealed with clay on both ends using a solder wick and wax. For 7 T DNP samples, 20-60 uL of sample is pipetted into a teflon sample cup. KBr is added to the samples to ensure the sample sticks to the tube. The sample tube is sealed with a teflon piece.

Q-Band EPR experiments were performed at 50 K on 5 mM TetraTrityl, 200 μM TetraTrityl, and 20 mM MonoTrityl in anhydrous toluene. 5 mM TetraTrityl in d_8-toluene were also tested at 50 K, and 5 mM TetraTrityl in anhydrous toluene was additionally tested at 30 K. For all samples, the concentrations mentioned are by default the radical concentration and not the unpaired electron concentration, unless otherwise specified.

Field-swept echo-detected EPR, nutation, and T_m experiments were performed on all samples. Meanwhile, T_{1e} interpulse delay-dependent field swept echo-detected EPR were performed on most samples. Echo-detected experiments used a 90°-180° pulse scheme. No phase cycling was used for Q-Band echo-detected EPR experiments, and a 4-step phase cycling used in T_{1e} experiments. Pulse lengths used for experiments were matched to the desired flip angle according to the determined nutation times, documented in Table S5 with some plotted examples in Figure S11 and referred to a 180° pulses at a given field. Attenuation refers to the power attenuation of the EPR spectrometer, where lower numbers refer to less attenuation and higher numbers refer

to greater attenuation.

^{1}H DNP and pulsed EPR experiments were performed at 6.9 T field using the 5 mM TetraTrityl, 1 mM TetraTrityl, and 20 mM MonoTrityl samples in anhydrous toluene, 5 mM MonoTrityl in 70:27.5:2.5 toluene-d_8:chloroform:anhydrous toluene, and 20 mM Trityl-OX063 in 78:14:8 DMSO:D_2O:H_2O. 5 mM TetraTrityl was measured at 60 K and 100 K, 1 mM TetraTrityl was measured at 60 K, and the MonoTrityl and Trityl-OX063 samples were measured at 20 K.

Frequency-swept DNP profiles and T_{1H} were measured for these samples. The DNP enhancement as a function of microwave power and DNP buildup time was acquired with 5 mM TetraTrityl. EPR experiments at 7 T were performed using a 90°-90° pulse scheme using incoherent pulses.

Fully quantum mechanical simulations of DNP and EPR processes were performed using the SpinEvolution simulation package mimicking experimental conditions at 50 K and 6.9 T.[33,22] T_{1e} and T_m parameters were taken from Q-Band EPR experiments at 50 K. Trityl-OXO63's rhombic g values of [2.0034 2.0031 2.0027] were used[34] for all simulations unless otherwise stated. The point dipole approximation is used for all spin dynamics calculations. The g-tensor Euler angles were chosen differently for different electron spins because of the flexibility of the linker. For all simulations, the Euler angles for the g-tensor for e_1, e_2, e_3, and e_4 are (0, 0, 0), (20, 30, 0), (40, 60, 0), and (60, 90, 0), respectively. Powder averaging was done using 50 (α, β) angles following the Lebedev scheme for weighted orientation distributions. The e_1-^{1}H distance is 6 Å in all cases unless otherwise specified-this distance is taken as a reasonable value given the average methyl-electron distance in the DFT-optimized structure is between 5.5 and 6.3 Å. Low microwave power (corresponding to a Rabi frequency between 50-200 kHz) was used to mimic experimental conditions.

Acknowledgement

We acknowledge the invaluable funding received from the National Science Foundation Grant CHE CMI 2004217 and the National Institute of General Medical Sciences MIRA Grant (Project 5R35GM136411-04) for the development of the dual DNP-EPR instrumentation. Synthesis of Monotrityl and TetraTrityl was supported by the Russian Ministry of Science and Higher Education grant to V.M.T and E.G.B. (14.W03.31.0034).Contribution from AE was supported by Tamkeen under the NYU Abu Dhabi Research Institute grant CG008. The authors thank Dr. Kan Tagami for the help with 7 T DNP experiments and Vishnu Vijayan and Dr. Tom Casey for their help with EPR measurements. The authors give special thanks to Celeste Tobar for helping run CW EPR measurements of TetraTrityl (Figure S4) and Dr. Quentin Stern for fruitful discussion and analytical Matlab calculations of e-e dipolar coupling distributions (Figure S15). The authors also thank Dr. Alexander Maryasov for fruitful discussion.

Supporting Information Available

Additional data and methods for experiments, simulations, and analytical calculations given.

References

(1) Bertarello, A.; Berruyer, P.; Artelsmair, M.; Elmore, C. S.; Heydarkhan-Hagvall, S.; Schade, M.; Chiarparin, E.; Schantz, S.; Emsley, L. In-Cell Quantification of Drugs by Magic-Angle Spinning Dynamic Nuclear Polarization NMR. *144*, 6734–6741, Publisher: American Chemical Society.

(2) Lerche, M. H.; Meier, S.; Jensen, P. R.; Hustvedt, S.-O.; Karlsson, M.; Duus, J. ; Ardenkjær-Larsen, J. H. Quantitative dynamic nuclear polarization-NMR on blood plasma for assays of drug metabolism. *24*, 96–103, _eprint: https://onlinelibrary.wiley.com/doi/pdf/10.1002/nbm.1561.

(3) Masion, A.; Alexandre, A.; Ziarelli, F.; Viel, S.; Santos, G. M. Dynamic Nuclear Polarization NMR as a new tool to investigate the nature of organic compounds occluded in plant silica particles. *7*, 3430, Number: 1 Publisher: Nature Publishing Group.

(4) Pourpoint, F.; Templier, J.; Anquetil, C.; Vezin, H.; Trébosc, J.; Trivelli, X.; Chabaux, F.; Pokrovsky, O. S.; Prokushkin, A. S.; Amoureux, J.-P.; Lafon, O.; Derenne, S. Probing the aluminum complexation by Siberian riverine organic matter using solid-state DNP-NMR. *452*, 1–8.

(5) Kaminker, I.; Barnes, R.; Han, S. Arbitrary waveform modulated pulse EPR at 200GHz. *279*, 81–90.

(6) Equbal, A.; Tagami, K.; Han, S. Pulse-Shaped Dynamic Nuclear Polarization under Magic-Angle Spinning. *10*, 7781–7788, Publisher: American Chemical Society.

(7) J. Kubicki, D.; Casano, G.; Schwarzwälder, M.; Abel, S.; Sauvée, C.; Ganesan, K.; Yulikov, M.; J. Rossini, A.; Jeschke, G.; Copéret, C.; Lesage, A.; Tordo, P.; Ouari, O.; Emsley, L. Rational design of dinitroxide biradicals for efficient cross-effect dynamic nuclear polarization. *7*, 550–558, Publisher: Royal Society of Chemistry.

(8) Lilly Thankamony, A. S.; Wittmann, J. J.; Kaushik, M.; Corzilius, B. Dynamic nuclear polarization for sensitivity enhancement in modern solid-state NMR. *102-103*, 120–195.

(9) Wenckebach, W. T. Dynamic nuclear polarization via the cross effect and thermal mixing: A. The role of triple spin flips. *299*, 124–134.

(10) Wenckebach, W. T. Dynamic nuclear polarization via the cross effect and thermal mixing: B. Energy transport. *299*, 151–167.

(11) Bussandri, S.; Shimon, D.; Equbal, A.; Ren, Y.; Takahashi, S.; Ramanathan, C.; Han, S. P1 center electron spin clusters are prevalent in type Ib diamond. `http://arxiv.org/abs/2311.05396`.

(12) Dobrinets, I. A.; Vins, V. G.; Zaitsev, A. M. *HPHT-Treated Diamonds: Diamonds Forever*; Springer Series in Materials Science; Springer Berlin Heidelberg, Vol. 181.

(13) Nir-Arad, O.; Shlomi, D. H.; Manukovsky, N.; Laster, E.; Kaminker, I. Nitrogen Substitutions Aggregation and Clustering in Diamonds as Revealed by High-Field Electron Paramagnetic Resonance.

(14) Equbal, A.; Li, Y.; Tabassum, T.; Han, S. Crossover from a Solid Effect to Thermal Mixing 1H Dynamic Nuclear Polarization with Trityl-OX063. *11*, 3718–3723, Publisher: American Chemical Society.

(15) Li, Y.; Equbal, A.; Tabassum, T.; Han, S. 1H Thermal Mixing Dynamic Nuclear Polarization with BDPA as Polarizing Agents. *11*, 9195–9202, Publisher: American Chemical Society.

(16) Shimon, D.; Cantwell, K. A.; Joseph, L.; Williams, E. Q.; Peng, Z.; Takahashi, S.; Ramanathan, C. Large Room Temperature Bulk DNP of 13C via P1 Centers in Diamond. *126*, 17777–17787, Publisher: American Chemical Society.

(17) Can, T. V.; Caporini, M. A.; Mentink-Vigier, F.; Corzilius, B.; Walish, J. J.; Rosay, M.;

Maas, W. E.; Baldus, M.; Vega, S.; Swager, T. M.; Griffin, R. G. Overhauser effects in insulating solids. *141*, 064202, Publisher: American Institute of Physics.

(18) Ghosh, R.; Xiao, Y.; Kragelj, J.; Frederick, K. K. In-Cell Sensitivity-Enhanced NMR of Intact Viable Mammalian Cells. *143*, 18454–18466, Publisher: American Chemical Society.

(19) Corzilius, B.; Andreas, L. B.; Smith, A. A.; Ni, Q. Z.; Griffin, R. G. Paramagnet induced signal quenching in MAS–DNP experiments in frozen homogeneous solutions. *240*, 113–123.

(20) Lange, S.; Linden, A. H.; Akbey, ; Trent Franks, W.; Loening, N. M.; Rossum, B.-J. v.; Oschkinat, H. The effect of biradical concentration on the performance of DNP-MAS-NMR. *216*, 209–212.

(21) Bretschneider, M.; Spindler, P. E.; Rogozhnikova, O. Y.; Trukhin, D. V.; Endeward, B.; Kuzhelev, A. A.; Bagryanskaya, E.; Tormyshev, V. M.; Prisner, T. F. Multiquantum Counting of Trityl Radicals. *11*, 6286–6290, Publisher: American Chemical Society.

(22) Veshtort, M.; Griffin, R. G. SPINEVOLUTION: A powerful tool for the simulation of solid and liquid state NMR experiments. *178*, 248–282.

(23) Golysheva, E. A.; Smorygina, A. S.; Dzuba, S. A. Double Electron–Electron Resonance vs. Instantaneous Diffusion Effect on Spin-Echo for Nitroxide Spins Labels.

(24) Salikhov, K. M.; Dzuba, S. A.; Raitsimring, A. M. The theory of electron spin-echo signal decay resulting from dipole-dipole interactions between paramagnetic centers in solids. *42*, 255–276.

(25) Dzuba, S.; Golovina, Y.; Tsvetkov, Y. Echo-Induced EPR Spectra of Spin Probes as a Method for Identification of Glassy States in Biological Objects. *101*, 134–138.

(26) Gast, P.; Mance, D.; Zurlo, E.; L. Ivanov, K.; Baldus, M.; Huber, M. A tailored multi-frequency EPR approach to accurately determine the magnetic resonance parameters of

dynamic nuclear polarization agents: application to AMUPol. *19*, 3777–3781, Publisher: Royal Society of Chemistry.

(27) Radaelli, A.; Yoshihara, H. A. I.; Nonaka, H.; Sando, S.; Ardenkjaer-Larsen, J. H.; Gruetter, R.; Capozzi, A. 13C Dynamic Nuclear Polarization using SA-BDPA at 6.7 T and 1.1 K: Coexistence of Pure Thermal Mixing and Well-Resolved Solid Effect. *11*, 6873–6879, Publisher: American Chemical Society.

(28) Wenckebach, W. T.; Quan, Y. Monte Carlo study of the spin-spin interactions between radicals used for dynamic nuclear polarization. *326*, 106948.

(29) Wenckebach, W. T.; Capozzi, A.; Patel, S.; Ardenkjær-Larsen, J. H. Direct measurement of the triple spin flip rate in dynamic nuclear polarization. *327*, 106982.

(30) Case, D. A.; Aktulga, H. M.; Belfon, K.; Ben-Shalom, I.; Brozell, S. R.; Cerutti, D. S.; Cheatham III, T. E.; Cruzeiro, V. W. D.; Darden, T. A.; Duke, R. E.; others, *Amber 2021*; University of California, San Francisco.

(31) Asanbaeva, N. B.; Novopashina, D. S.; Rogozhnikova, O. Y.; Tormyshev, V. M.; Kehl, A.; Sukhanov, A. A.; Shernyukov, A. V.; Genaev, A. M.; Lomzov, A. A.; Bennati, M.; Meyer, A.; Bagryanskaya, E. G. 19F electron nuclear double resonance (ENDOR) spectroscopy for distance measurements using trityl spin labels in DNA duplexes. *25*, 23454–23466, Publisher: The Royal Society of Chemistry.

(32) Tormyshev, V. M.; Genaev, A. M.; Sal'nikov, G. E.; Rogozhnikova, O. Y.; Troitskaya, T. I.; Trukhin, D. V.; Mamatyuk, V. I.; Fadeev, D. S.; Halpern, H. J. Triarylmethanols with Bulky Aryl Groups and the NOESY/EXSY Experimental Observation of a Two-Ring-Flip Mechanism for the Helicity Reversal of Molecular Propellers. *2012*, 623–629, _eprint: https://onlinelibrary.wiley.com/doi/pdf/10.1002/ejoc.201101243.

(33) Equbal, A.; Jain, S. K.; Li, Y.; Tagami, K.; Wang, X.; Han, S. Role of electron spin dynamics and coupling network in designing dynamic nuclear polarization. *126-127*, 1–16.

(34) Mentink-Vigier, F.; Mathies, G.; Liu, Y.; Barra, A.-L.; A. Caporini, M.; Lee, D.; Hediger, S.; Griffin, R. G.; Paëpe, G. D. Efficient cross-effect dynamic nuclear polarization without depolarization in high-resolution MAS NMR. *8*, 8150–8163, Publisher: Royal Society of Chemistry.

TOC Graphic

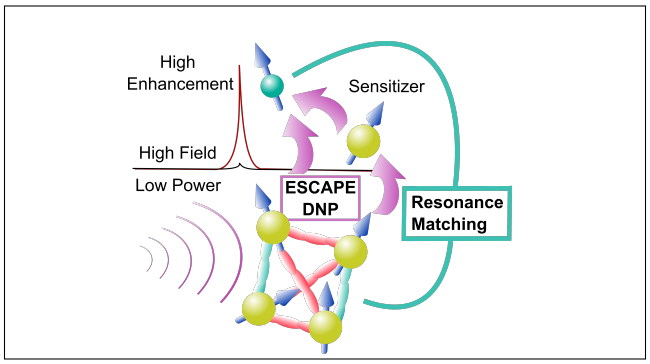
High
Enhancement
Sensitizer
High Field
Low Power
ESCAPE
DNP
Resonance
Matching